Chapter 7

Transformation from CIT-13 to CIT-5

In this chapter, the spontaneous transformation of Ge-CIT-13 into Ge-CIT-5 is discussed. The influence of the type of parent Ge-CIT-13 on the transformation rate and the role of moisture in the transformation are elucidated. The resultant Ge-CIT-5 is characterized and compared to CIT-5 synthesized using the methylsparteinium OSDA. Similar layered germanosilicates containing Ge-rich *d*4*r* units are also investigated in terms of transformability upon exposure to moisture in ambient air as a comparison to the Ge-CIT-13.

7.1. Introduction

CIT-5 (CFI) is an extra-large-pore high-silica zeolite having one-dimensional 14-ring channels.[131] As mentioned in Chapter V, since its discovery, the catalysis over extra-large-pore zeolites has been extensively studied together with other 14-pore aluminosilicate and borosilicate such as UTD-1, SSZ-53, and SSZ-59.[134-135, 139] Unfortunately, the only synthetic pathway for CIT-5 that has been reported was the recipe using N-methylsparteinium as the OSDA which is very expensive and hard to obtain. In 2017, the scientific community saw news regarding the sudden nationwide scarcity of sparteine in the market for an unknown reason.[179] Since the use of sparteine is the only way to obtain CIT-5, the market availability of CIT-5 automatically will be always open to questions unless any stable sources of sparteine are secured.

CIT-13 is structurally related not only to IM-12, but also to CIT-5. The two frameworks share the same *cfi*-layer structure and have 14-ring pores. In CIT-13 and CIT-5, the *cfi*-layers are connected via *d*4*r* units and double zigzag chains, respectively. Surprisingly, calcined germanosilicate CIT-13 slowly transformed into another germanosilicate having a CFI topology under a general lab atmosphere. This transformation was so slow that sometimes it took many months. There has been a consensus in the scientific community that exposing calcined germanosilicate to moisture in ambient atmosphere is not desirable in terms of preservation of structures.[158, 180]

Intentionally exploiting the chemical lability of germanium T-sites in zeolitic frameworks has begotten many transformation and postsynthesis protocols, such as the ADOR method.[181] However, in those procedures, germanosilicates should be submerged in liquid phases such as weak or strong acids.[118, 161, 182] The transformation of Ge-CIT-13 into Ge-CIT-5 can be accomplished without such wet procedures. The key stage of the CIT-13-to-5 transformation was sorption of moisture from the atmosphere. In this regard, this transformation is like the moisture-mediated transformation of VPI-5 to $AlPO_4$-8 at elevated temperature.[127, 183]

In this chapter, the role of sorbed water within the pore systems of germanosilicates will be discussed. The relationship between the rate of transformation and the nature of the parent Ge-CIT-13 will be also investigated. The resultant Ge-CIT-5 will be also compared to pure-silica CIT-5 synthesized from the original recipe. Also, the structure evolutions of other germanosilicates will be discussed.

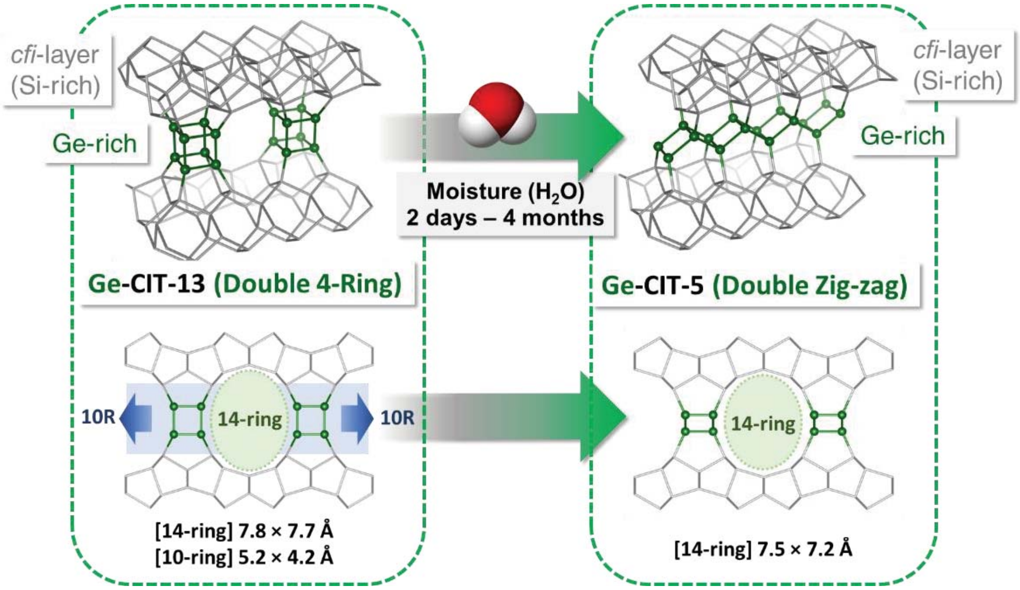

Figure 7.1. Transformation from Ge-CIT-13 to Ge-CIT-5

7.2. Experimental

7.2.1. Preparation of Parent Ge-CIT-13

Parent Ge-CIT-13 molecular sieves were synthesized according to the methods explained in the previous chapter. Ge-CIT-13 samples were prepared on the basis of the two protocols: the fluoride recipes and the hydroxide recipes. The gel compositions are given in the previous chapter. The target Si/Ge ratios of Ge-CIT-13 parent materials were in the range of 3.5–5.5. This range of Si/Ge ratios could be achieved by controlling the gel Si/Ge ratios in the range of 2.5–4.0. An empirical correlation between the gel Si/Ge ratio and the Si/Ge ratio of the resultant CIT-13 is given in Figure B1. Calcination was performed at 580 °C for 6 hours to remove occluded organics.

7.2.2. Transformation of Ge-CIT-13 to Ge-CIT-5

The transformation from Ge-CIT-13 to Ge-CIT-5 requires no specific procedure because it starts immediately after calcination. Just by leaving calcined Ge-CIT-13, the transformation was automatically achieved under an ambient condition (room temperature and relative humidity of 30 %). To keep the humidity constant, in this work, the transformation was conducted in a small chamber where the internal temperature and humidity were monitored and controlled (30 % relative humidity at 25 °C).

7.2.3. Preparation of Reference Sparteine-CIT-5

Pure-silica reference CIT-5 was prepared from hydrothermal synthesis using N-methylsparteinium hydroxide as the OSDA on the basis of protocols reported by our group.[131-132, 184] First, 50 mmol of (-)-Sparteine (Aldrich) was dissolved in 150 ml of chloroform. The reaction mixture was cooled down in an ice bath, and 70 mmol of methyl iodide was added dropwise for 30 min. The reaction was undergone at room temperature for 72 hour under continuous stirring in the dark. The product was crystallized by adding excess diethyl ether, and collected by filtration. Recrystallization was performed using isopropanol and ethyl acetate. The final product was dried in vacuum at room temperature. The obtained bright yellow N-methylsparteinium iodide salt was converted to its hydroxide-form by a typical ion-exchange procedure using DOWEX™ Monosphere™ 550A ion-exchange resin (Dow Chemical). The detailed procedure for the ion-exchange was described in the previous chapter. If (-)-sparteine sulfate salt was provided as the starting material, free (-)-sparteine can be obtained by extraction using 3 M NaOH aqueous solution.[184]

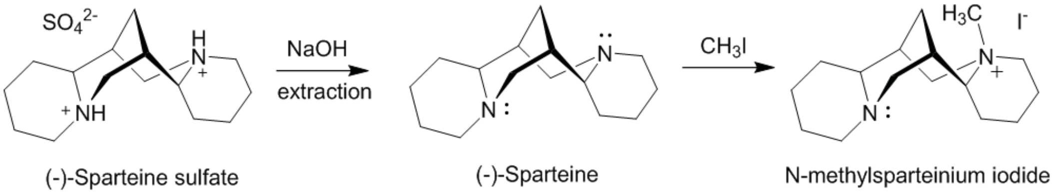

Figure 7.2. Reaction scheme for the preparation of N-methylsparteinium OSDA.

The gel composition used for the hydrothermal synthesis of pure-silica sparteine-CIT-5 was 1.0 SiO_2 : 0.10 LiOH : 0.24 MSpaOH : 40 H_2O where MSpaOH denotes N-methylsparteinium hydroxide. A desired amount of lithium hydroxide monohydrate ($LiOH \cdot H_2O$, Sigma-Aldrich, 98.5–101.5 %) was dissolved in a desired amount of MSpaOH aqueous solution. Colloidal silica Ludox® HS-30 (Sigma-Aldrich) was added, and the mixture was stirred for 24 hours. Lastly, distilled water was added to the gel to achieve the desired gel composition. The final gel was charged into a 23-mL PTFE-lined Parr steel autoclave. The crystallization was performed at 175 °C for 7 days in a static oven. The resultant product was washed with distilled water and acetone, and dried at 100 °C. Calcination was performed at 580 °C for 6 hours under an air flow. For the rest of this work, this reference sample based on the original recipe of CIT-5 is referred to as Spa-CIT-5 to avoid confusion.

7.2.4. Preparation of IM-12, JLG-18, and ITQ-22

Germanosilicates IM-12 (UTL), JLG-18 (ITH), and ITQ-22 (IWW) were prepared on the basis of protocols reported in the literature.[116, 146, 185] Detailed descriptions for the synthesis of IM-12 are provided in the previous chapter.

JLG-18 was synthesized using commercially available N,N,N’,N’-tetramethyl-1,6-hexanediamine (TMDA) as the OSDA.[185] In a desired amount of distilled water, TMDA (Sigma-Aldrich, 99%), tetraethyl orthosilicate (TEOS, Alfa Aesar, 98%), and germanium oxide (Strem, 99.999%) were added and homogenized for 24 hours. After that, a desired amount of ammonium fluoride (98%, Sigma-Aldrich) was added and stirred overnight. The final gel molar composition was x/(x+1) SiO_2 : 1/(x+1) GeO_2 : 7.0 TMDA : 1.40 NH_4F : 44 H_2O where x ($0.75 < x < 1$) is the gel Si/Ge molar ratio. The mixture was sealed in a PTFE-lined steel autoclave (Parr Instrument) and crystallized in a rotating or static oven at 175 °C for 1 week. The resultant product was washed with distilled water and acetone, and dried in a convection oven at 100 °C.

ITQ-22 was prepared using 1,5-bis-(methylpyrrolidinium)-pentane dibromide ($MPP^{2+}Br_2^-$) which can be synthesized from the S_N2 reaction between N-methylpyrrolidine and 1,5-dibromopentane.[146, 186] An excess amount of N-methylpyrrolidine (97%, Sigma-Aldrich, 25.5 g, 300 mmol) was dissolved in 350 ml of acetone in a round-bottom flask, and 23.0 g (100 mmol) of 1,5-dibromopentane (97%, Sigma-Aldrich) was added dropwise. The mixture was stirred under reflux for 48 hours and the solid product was collected by filtration. The product was washed with cool acetone and diethyl ether, and dried in a vacuum at room temperature. The ion-exchange and titration procedures were described in the previous chapter.

The gel composition used for the hydrothermal synthesis of ITQ-22 was 0.67 SiO_2 : 0.33 GeO_2 : 0.25 $MPP^{2+}(OH^-)_2$: 7.0 H_2O. A desired amount of germanium oxide was dissolved in a desired amount of $MPP^{2+}(OH^-)_2$ aqueous solution. TEOS was added, and the mixture was stirred for 24 hours. Lastly, excess water was evaporated under an air flow. The final gel was charged into a 23-mL PTFE-lined Parr steel autoclave. The crystallization was performed at 175 °C for 7 days in a static oven. The resultant product was washed with distilled water and acetone, and dried at 100 °C. Calcination was performed at 580 °C for 6 hours under an air flow.

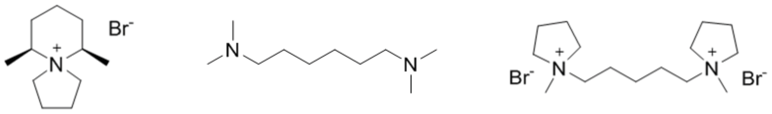

For UTL For ITH For IWW

Figure 7.3. Structures of OSDA used to synthesize germanosilicates.

7.2.5. Characterization

PXRD patterns were acquired using a Rigaku MiniFlex II benchtop diffractometer using Cu Kα radiation (λ = 1.54184 Å) to assess the crystal structure and crystallinity of the products. Thermogravimetric analysis (TGA) was performed using a PerkinElmer STA6000 instrument under a nitrogen flow of 20 mL min^{-1}. Morphology and elemental composition were studied using a Zeiss 1550VP FE-SEM equipped with an Oxford X-Max SDD X-ray EDS. Pore volumes and pore-size information of microporous materials were studied based on Ar adsorption isotherms obtained using a Quantachrome Autosorb iQ at 87.45 K. ^{1}H, ^{27}Al and ^{29}Si MAS solid-state NMR spectra of samples were obtained using a Bruker Avance 500 MHz spectrometer with carrier frequencies of 499.843, 130.287 and 99.305 MHz, respectively. A 4-mm zirconia rotor with a Kel-F cap was charged with 50–100 mg of as-made or freshly calcined sample. The MAS rates were 8 kHz both for ^{1}H-^{29}Si CP and ^{1}H-decoupled ^{29}Si Bloch-decay experiments, and 12 kHz for ^{27}Al experiments.

7.3. Results and Discussion

7.3.1. Rate of Transformation

The transformation from Ge-CIT-13 to Ge-CIT-5 is a very slow process which typically takes several weeks or even several months. The rate of transformation depends on many factors. Among them, the two most important factors determining the rate of transformation were the germanium content of the parent Ge-CIT-13 and the synthetic recipe of which the parent germanosilicate is based.

In this chapter, synthetic and material information of the parent Ge-CIT-13 is denoted as Ge-CIT-13/*x*[*y*], where *x* is the mineralizer (*x* = F or OH) used to synthesize the sample, and *y* denotes the EDS Si/Ge ratio of the sample. For example, Ge-CIT-13/F[4.5] means a Ge-CIT-13 sample of Si/Ge = 4.5 which was synthesized from the fluoride media.

The progress of transformation can be monitored on the basis of diffraction patterns. As a result of the transformation, the interlayer distance among the *cfi*-layers decreases. This interlayer contraction engenders a discernable shift of the (200) diffraction peak of PXRD pattern of transforming material. For Ge-CIT-13, the peak position of (200) diffraction is at $2\theta = 6.44°$ ($d_{200} = 13.7$ Å). This interlayer diffraction peak of the parent material moves toward a higher angle until it reaches $2\theta = 6.9–7.0°$ ($d_{200} = 12.6–12.8$ Å) which corresponds to the theoretical (200) diffraction peak position of the framework CFI which is at $2\theta = 6.93°$ ($d_{200} = 12.7$ Å). The (110) diffraction peak also moves from 7.16° to 7.32°, and this shift of the (110) peak is crystallographically consistent with the shift of (200) peak.

The CFI framework shows its characteristic three diffraction peaks in the range of $2\theta = 12–15°$; three peaks at 12.2°, 12.9°, and 13.9° are corresponding to the (301), (002), and (400) diffractions of the CFI framework.[16] The initial framework *CTH also show the corresponding diffractions in the same region of 2θ at 11.6°, 12.8°, and 12.9°, but practically only one or two diffractions are observed because the (301) diffraction at 11.6° is often very weak and because the latter two peaks overlap one another at the same angle of 2θ.

Figure 7.4 illustrates this slow transformation of Ge-CIT-13/F[4.31] to Ge-CIT-5. The interlayer (200) diffraction of the freshly calcined Ge-CIT-13 moved slowly from $2\theta = 6.40°$ to 7.02° during 85 days of exposure to the ambient air. Three diffraction peaks of (301), (002), and (400) also appeared in the range of $2\theta = 12–15°$. This pattern showed no further evolution for the next 700 days. The final diffraction pattern matched well with the PXRD diffraction pattern of the reference pure-silica Spa-CIT-5. To the best of my knowledge, this is the first inter-framework germanosilicate transition occurring at the room temperature. Ge-CIT-5, the final material, is also the first CFI-type extra-large-pore germanosilicate which is structurally stable under the ambient humidity. Some more examples of transformations of Ge-CIT-13/F[*y*] (*y* = 4.11–4.65) are provided in Figures B13–B16, Appendix B.

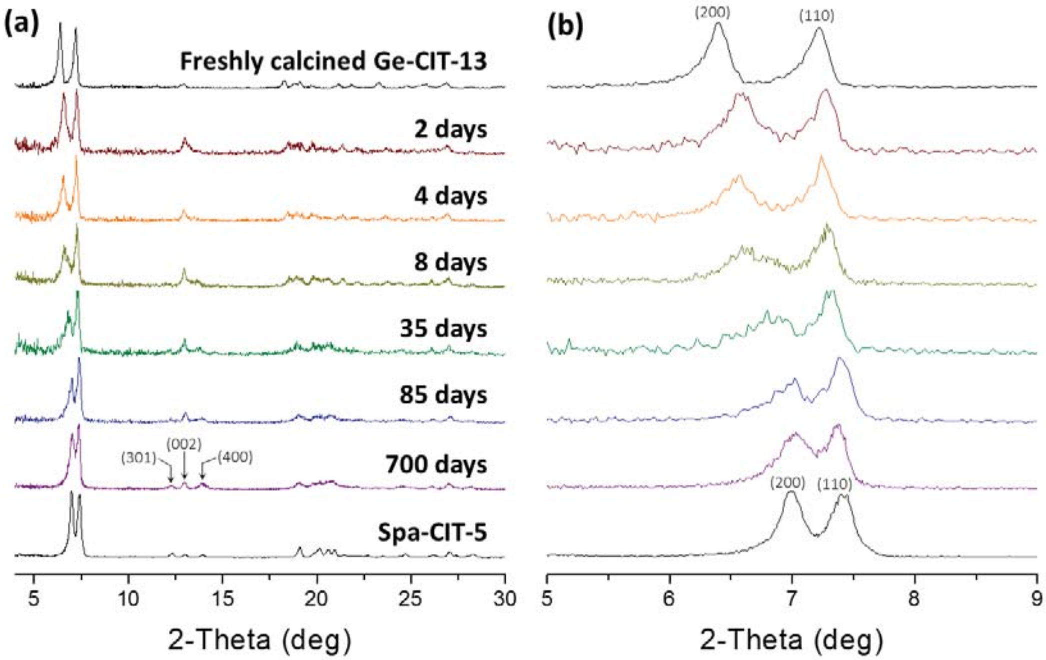

Figure 7.4. Transformation of Ge-CIT-13/F (Si/Ge = 4.31) to Ge-CIT-5 over time observed on the basis of PXRD patterns in 2-theta scanning ranges of (a) 4–30° and (b) 5–9°.

Increasing the germanium contents of parent Ge-CIT-13 greatly accelerated the rate of transformation. Figure 7.5 shows an analogous transformation of Ge-CIT-13/F[3.87] having more germanium in the framework than Ge-CIT-13/F[4.31]. This high-germanium

Ge-CIT-13 transformed just within 12 days, much faster than the Ge-CIT-13/F[4.31] which took 85 days. Interestingly, 3 days after calcination, Ge-CIT-13/F[3.87] showed two distinct peaks at 6.68° and 6.90° which may correspond to the (200) interlayer diffractions of intermediate stages. This observation clearly supports that there are two types of crystals in some transforming batches. The latter peak at 6.90° must be corresponding to the (200) peak of the CFI framework which is the final phase of the transformation. The former peak located between the (200) peaks of Ge-CIT-13 (6.44°) and Ge-CIT-5 (6.93°) is presumably the interlayer diffraction of hydrated Ge-CIT-13 phase. Similar behaviors were observed in the case of Ge-CIT-13/F[4.65] shown in Figure B16. The origin of this inhomogeneous transformation remains unknown to me. On the other hand, Ge-CIT-13 having Si/Ge ratios

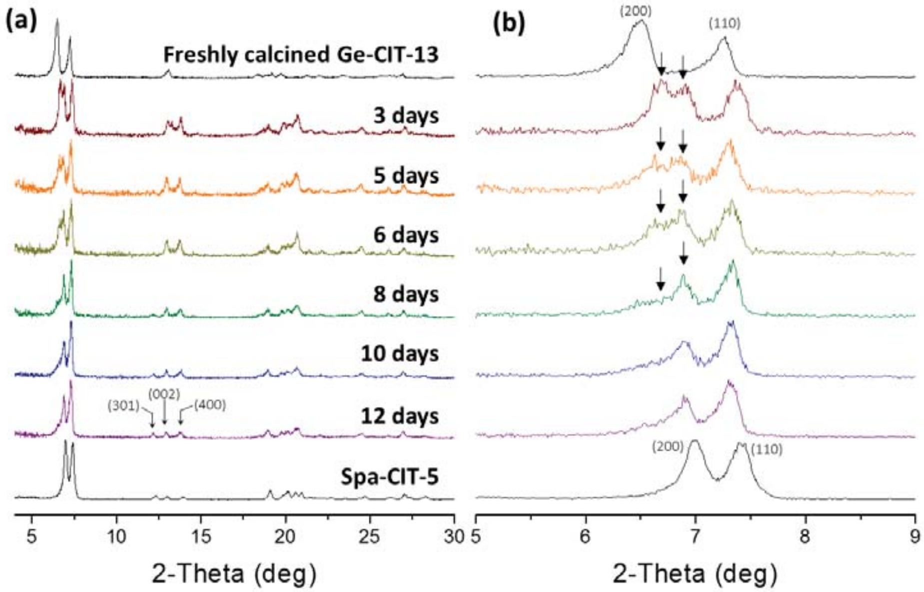

Figure 7.5. Transformation of Ge-CIT-13/F (Si/Ge = 3.87) to Ge-CIT-5 over time observed on the basis of PXRD patterns in 2-theta scanning ranges of (a) 4–30° and (b) 5–9°.

higher than 6 showed an extremely slow rate of transformation. Figure 7.6. illustrates the structural change of Ge-CIT-13/F[6.38] on the basis of PXRD patterns. This Ge-CIT-13 was not transformed even after 895 days of exposure to ambient humidity. No significant change was observed during the last 140 days of transformation. This result provides further evidence that the Si/Ge ratio of parent Ge-CIT-13 is one of the most important factor that determines the rate of transformation.

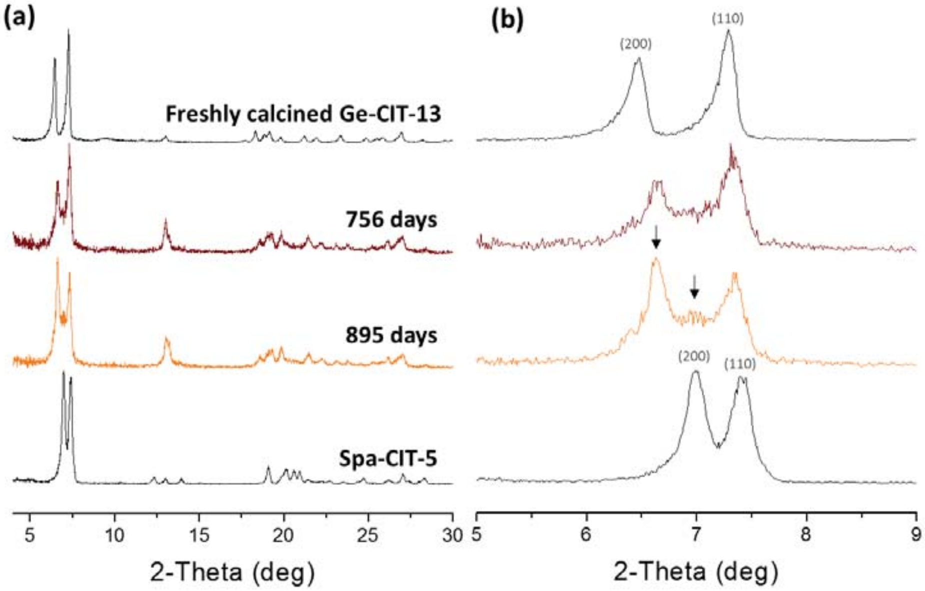

Figure 7.6. Transformation of Ge-CIT-13/F (Si/Ge = 6.38) to Ge-CIT-5 over time observed on the basis of PXRD patterns in 2-theta scanning ranges of (a) 4–30° and (b) 5–9°.

Ge-CIT-13/OH samples synthesized without use of fluoride showed a much faster transformation. While Ge-CIT-13/F[4.31] took 85 days (ca. 3 months) for the transformation as shown above, Ge-CIT-13/OH[4.33] having a similar germanium content was transformed into the corresponding Ge-CIT-5 within just 8 days under the same temperature and humidity, as shown in Figure 7.7. As expected, the combination of low Si/Ge ratio and hydroxide-based synthesis immensely accelerated the transformation. Figure 7.8 depicts the transformation of Ge-CIT-13/OH[3.88] which is completed in 2 days. No sign of CIT-13 is left after the second day of the transformation, and all diffractions well matched those of the reference Spa-CIT-5.

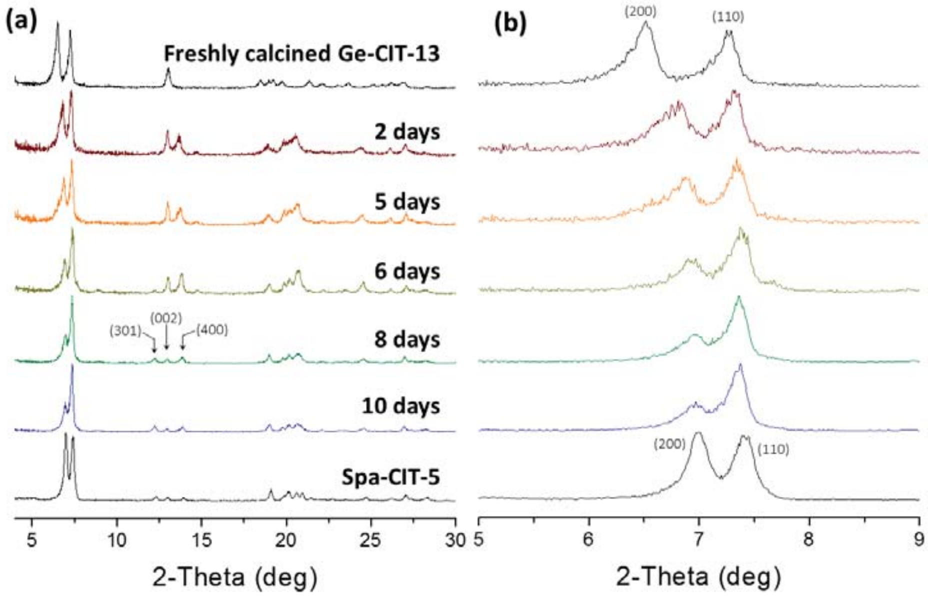

Figure 7.7 Transformation of Ge-CIT-13/OH (Si/Ge = 4.33) to Ge-CIT-5 over time observed on the basis of PXRD patterns in 2-theta scanning ranges of (a) 4–30° and (b) 5–9°.

I believe that this big difference in the rate of transformation in spite of similar Si/Ge ratios is related to the arrangement of germanium atoms within the *d*4*r* units of CIT-13 structure. It is known that fluoride anions can structure-direct the *d*4*r* units.[129, 187] This structure-directing ability of fluoride is particularly important for pure-silica syntheses of *d*4*r*-containing molecular sieves such as STW[188] or LTA.[62] But some *d*4*r*-containing germanosilicates (*e.g.*, ITH) can be prepared in both ways: with or without fluoride.[146, 175-176]

Ge-CIT-13 is also one of these cases. The inverse sigma transformation from Ge-rich CIT-13/OH[*y*] (y < 3.8) to CIT-14 will be discussed in the next chapter. This type of transformability strongly suggests the presence of Ge-O-Ge bonds in the *d*4*r* units.[118] I believe that the absence of fluoride promotes the formation of Ge-O-Ge bonds which can be hydrolyzed easier than Si-O-Ge bonds and that this preferred formation of Ge-O-Ge bonds is the main reason for the difference between the transformation rates of Ge-CIT-13/OH and Ge-CIT-13/F.

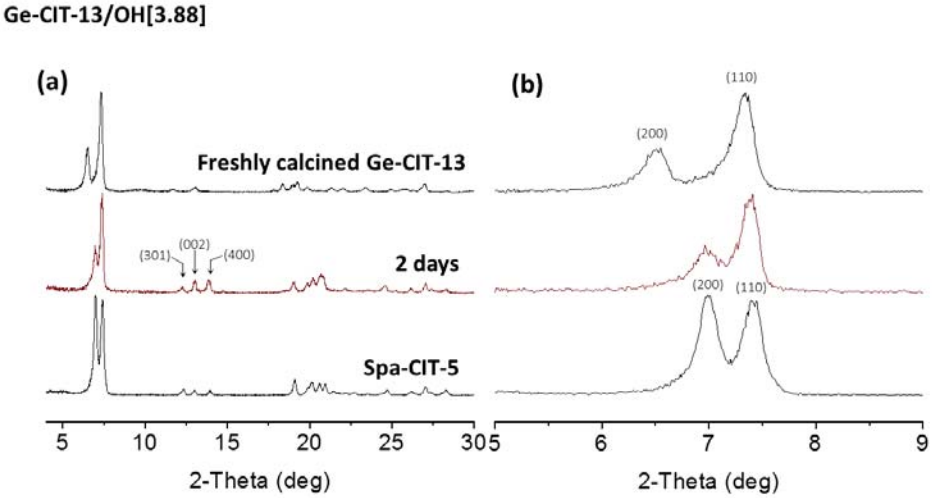

Figure 7.8. Transformation of Ge-CIT-13/OH (Si/Ge = 3.88) to Ge-CIT-5 over time observed on the basis of PXRD patterns in 2-theta scanning ranges of (a) 4–30° and (b) 5–9°.

7.3.2. Role of Sorbed Water within Pore System

The pith of the transformation from Ge-CIT-13 to Ge-CIT-5 is the formation of Ge-rich double-zigzag-chain (*dzc*) from arrays of *d*4*r* units. To achieve this transformation, dissociation and new formation of T-O-T bonds must occur. On the basis of the observations presented in the previous section, it can be deduced that the chemical lability of Ge-O bonds plays a crucial role in transformation. Ge-O bonds can be hydrolyzed very easily even by moisture in an ambient air. It has been pointed out many times that the low hydrothermal stability of most of the germanosilicate is originated from the hydrolysis of Ge-O bonds which significantly contribute to architectures of frameworks.[151, 154, 157-158] However, the hydrolysis of Ge-O bonds by occluded water is an essential part of the CIT-13-to-5 transformation. Indeed, the final Ge-CIT-5 after 4 months of exposure to ambient humidity possessed approximately 4.2 wt. % of water (see Figure B17).

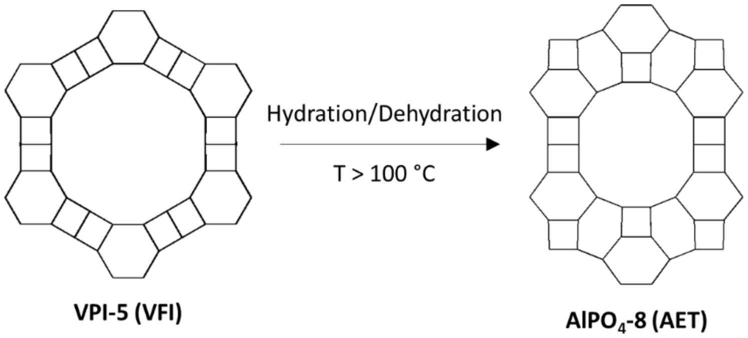

Figure 7.9. Transformation from VPI-5 to $AlPO_4$-8.

There is another inter-zeolitic transformation in which the role of sorbed water phase is essential: the transformation from VPI-5 (VFI) to $AlPO_4$-8 (AET). (see Figure 7.9) VPI-5 is the first synthetic extra-large-pore aluminophosphates-based molecular sieve discovered 32 years ago by Prof. Mark E. Davis who is my advisor.[124] VPI-5 transforms into $AlPO_4$-8 if moisture is present at an elevated temperature (> 100 °C).[125, 127] The hydration-dehydration of VPI-5 is the key process driving the transformation. The case of the transformation from Ge-CIT-13 to Ge-CIT-5 resembles the transformation from VPI-5 to $AlPO_4$-8 in regard of the necessity of moisture. One difference between these two inter-zeolitic transformations is temperature. Ge-CIT-13 transforms at room temperature.

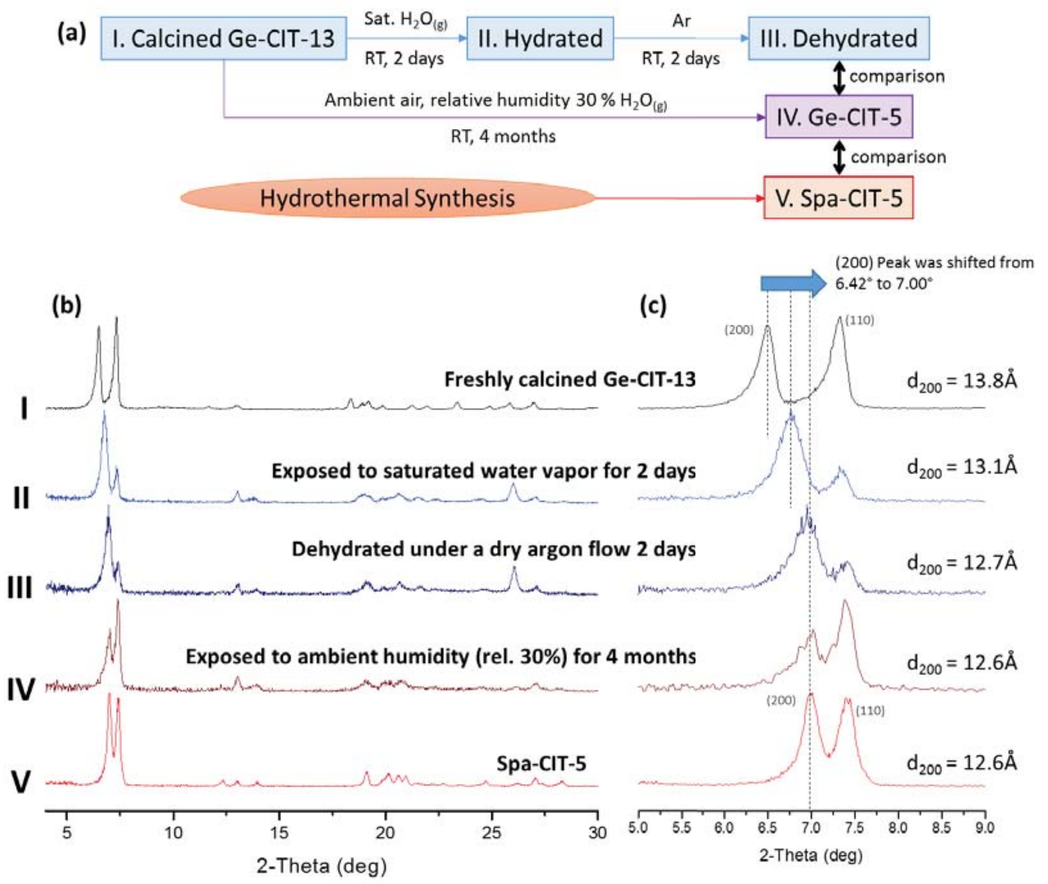

Figure 7.10. Accelerated transformation of Ge-CIT-13/F (Si/Ge = 4.31) to Ge-CIT-5: (a) design of experiment, (b) PXRD patterns in 2-theta scanning ranges of (b) 4–30° and (c) 5–9°.

To verify the role of sorbed water molecules within the pore system of CIT-13 in the transformation, a similar hydration/dehydration process was performed on Ge-CIT-13. Calcined Ge-CIT-13/F[4.31] was hydrated by exposing it to saturated water vapor for 2 days and subsequently dehydrated under a dry argon flow for another 2 days. This hydration/dehydration process was performed at room temperature. PXRD patterns were acquired at each stage to investigate structural evolution. The design of this experiment and related PXRD patterns are shown in Figure 7.10. Clearly, the interlayer distance of Ge-CIT-13/F[4.31] was decreased to 12.7 Å which corresponds to that of CIT-5. Extended hydration did not further decrease the interlayer distance of the germanosilicate (see Figure B17, Appendix B). However, the resultant material obtained in this way showed very low crystallinity, presumably due to disorder caused by larger amounts of sorbed water than in a usual ambient condition. The weak relative intensities of the (110) diffraction of PXRD profiles II and III indicate that a significant level of degree of disorder is generated along the b-axis (the direction perpendicular to the direction of the 14-ring main channel within the interlayer region).

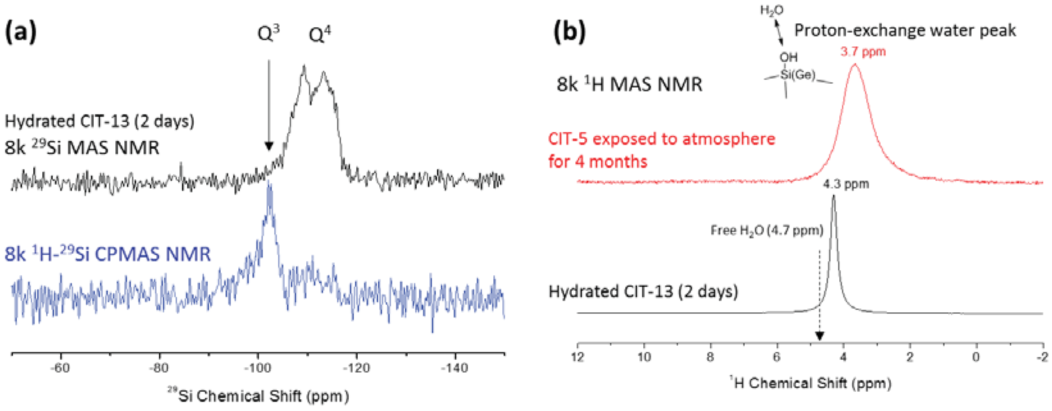

Figure 7.11. NMR spectra of hydrated Ge-CIT-13. (a) 8 kHz MAS ^{1}H-decoupled ^{29}Si solid-state NMR spectrum and ^{1}H-^{29}Si CP-MAS solid-state NMR spectrum of hydrated Ge-CIT-13/F[4.31] (II of Figure 7.10) and (b) 8 kHz MAS ^{1}H solid-state NMR spectra of sorbed water within Ge-CIT-5 produced by exposing Ge-CIT-13/F[4.31] to ambient humidity for 4 months (red, IV of Figure 7.10) and saturated water vapor for 2 days (black, II of Figure 7.10).

The hydrated germanosilicate (III of Figure 7.10) and sorbed water phase within its pore system were further studied on the basis of the solid-state ^{1}H and ^{29}Si NMR spectroscopy. The acquired spectra are illustrated in Figure 7.11. The ^{29}Si Bloch-decay NMR spectra (blue, Figure 7.11(a)) of hydrated Ge-CIT-13/F[4.31] give a pattern very similar to that of typical calcined Ge-CIT-13 shown in the previous chapter. But the Q^3-silanol (Si-OH) signal that appeared at -102.6 ppm in the ^{1}H-^{29}Si CP-MAS spectrum supports the presence of a small amount of hydrolyzed Si-O-Ge bonds.

It was also found that there is a continuous proton exchange between sorbed water phase and surface silanol groups in Ge-CIT-5 and hydrated Ge-CIT-13/F[4.31] on the basis of ^{1}H NMR spectra. The proton exchange between sorbed water phase and surface silanol groups can be evidenced by the upfield-shift of water signal in the proton NMR spectra.[189] Bulk pure water and silanol group shows their proton signal at 4.7 ppm and 1.9 ppm, respectively. For Ge-CIT-5 and hydrated Ge-CIT-13/F[4.31], the resonances of sorbed water within the pore systems of germanosilicates were detected at 3.7 ppm and 4.3 ppm, respectively. The line broadening of 3.7 ppm peak of the ^{1}H spectrum of Ge-CIT-5 from Ge-CIT-13/F[4.31] may be due to the strong dipole-dipole interaction among surface protons which could not be removed by MAS.[189] These signals which were broadened and shifted toward upper field support that the sorbed water phase and the surface silanol groups exchange protons.

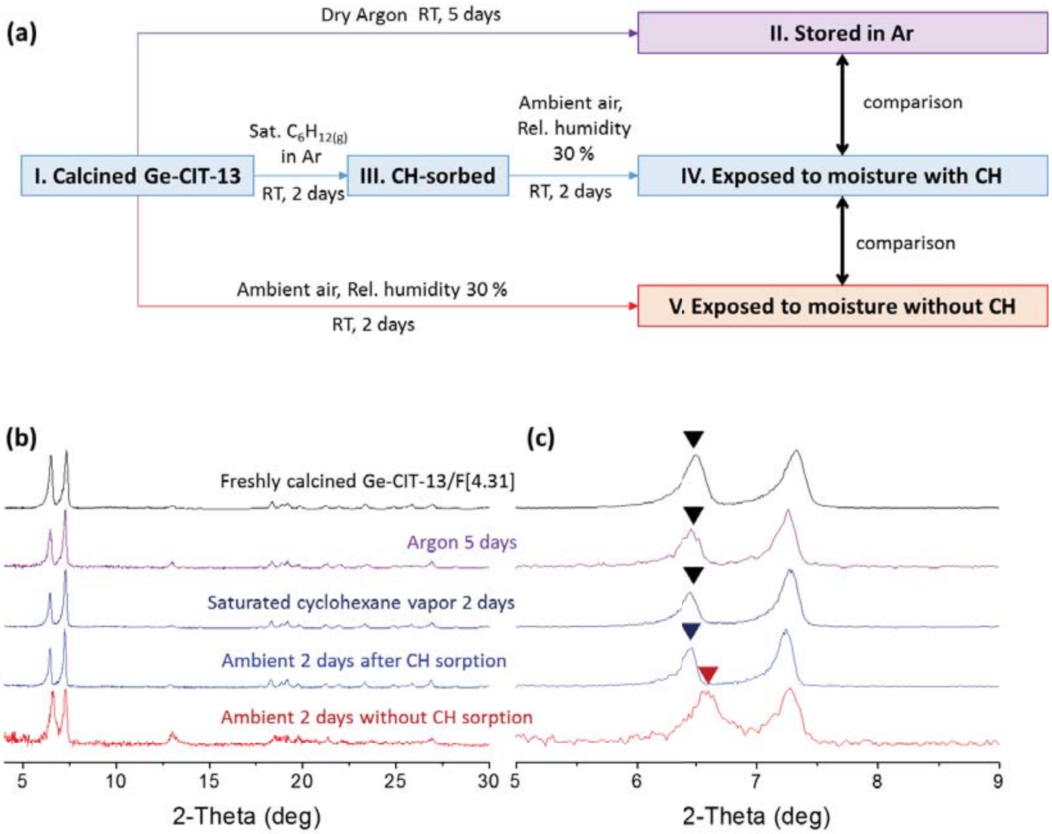

Figure 7.12. Inhibited transformation of Ge-CIT-13/F (Si/Ge = 4.31) to Ge-CIT-5 by excluding moisture from the system by argon and cyclohexane (CH): (a) design of experiment, and PXRD patterns in 2-theta scanning ranges of (a) 4–30° and (b) 5–9°.

On the other hand, isolating calcined Ge-CIT-13 from moisture inhibited or substantially decelerated the transformation. The design of experiment is illustrated in Figure 7.12(a). Firstly, freshly calcined dry Ge-CIT-13/F[4.31] was exposed to a dry argon (99.999%) flow for 5 days and a diffraction pattern was acquired, and compared to the case of ambient air exposure. No sign of structural evolution or degradation was found in the sample exposed to dry argon (II of Figure 7.12). However, the sample exposed to ambient air (30 % relative humidity) showed a noticeable decrease in the interlayer distance from 13.7 Å (2θ = 6.46°) to 13.4 Å (2θ = 6.6°) within just 2 days. (V of Figure 7.4)

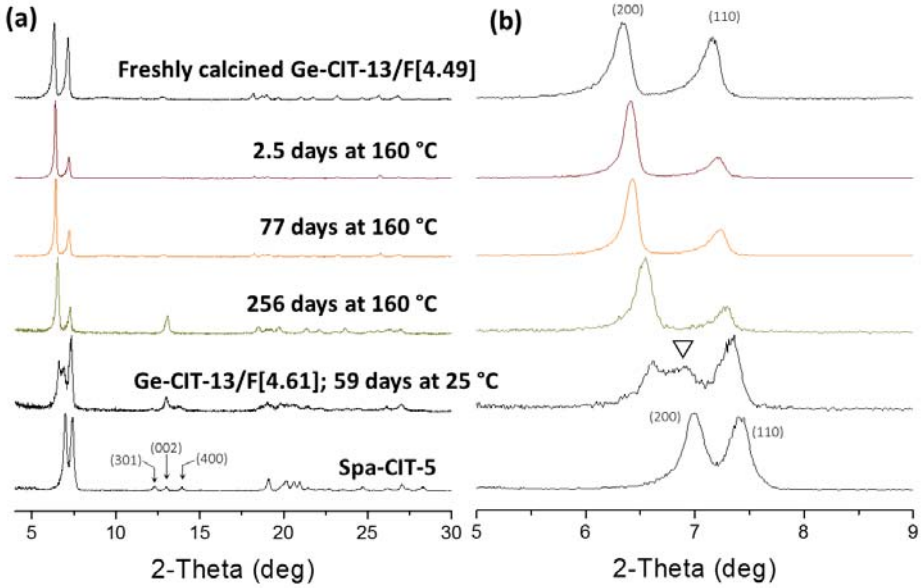

Figure 7.13. Structural change of Ge-CIT-13/F (Si/Ge = 4.49) at an elevated temperature (160 °C) over time observed on the basis of PXRD patterns in 2-theta scanning ranges of (a) 4–30° and (b) 5–9°.

Another portion of the same calcined Ge-CIT-13/F[4.31] was exposed to the saturated vapor of cyclohexane in dry argon at room temperature for 2 days. The vapor pressure of cyclohexane at 25 °C is 97.6 torr,[190] and the cyclohexane uptake of Ge-CIT-13 characterized by TGA was 7.5 wt. %. (TGA: not shown) Also, this cyclohexane-sorption did not cause any structural evolution of Ge-CIT-13. (III of Figure 7.12) After that, this Ge-CIT-13 having occluded cyclohexane in its pore system is exposed to ambient air of 30 % relative humidity for another 2 days. The PXRD pattern IV of Figure 7.12 clearly indicate that Ge-CIT-13 occluded with cyclohexane did not transform at all. The ^{1}H-^{13}C CP-MAS NMR and ^{1}H NMR spectra of cyclohexane-occluded Ge-CIT-13 (not shown) revealed that sorbed cyclohexane is still the majority species in Ge-CIT-13 and that sorption of water that can cause the transformation is substantially suppressed by the presence of hydrophobic cyclohexane. A barely visible and broad water signal was observed at 2.9 ppm which further shifted from 3.7 ppm of Ge-CIT-13 exposed to ambient humidity without cyclohexane. This inhibition experiment further evidences that moisture drives the transformation of Ge-CIT-13 to -5.

Lastly, the transformation was attempted at an elevated temperature higher than the boiling point of water. Calcined Ge-CIT-13/F[4.49] was placed in a convection oven at 160 °C, and its structural change was investigated for 256 days of high-temperature storage. PXRD patterns are shown in Figure 7.13. Ge-CIT-13/F[4.49] was barely transformed even after 256 days at 160 °C. Considering the fact that Ge-CIT-13/F[4.61] having higher Si/Ge ratio showed a sign of transformation after 59 days of ambient moisture exposure at room temperature, Ge-CIT-13/F[4.49] richer in germanium should have transformed faster than that—but it did not. The relative humidity of 30 % at room temperature (25 °C) is corresponding to the water vapor pressure of 7.1 torr.[190] The same air was circulated into the convection oven. Since the saturation vapor pressure of water at 160 °C is 4640 torr,[190] 7.1 torr is corresponding to a low relative humidity of 0.15 % at 160 °C at which liquid-phase water does not exist under a standard pressure (752 torr). So it can be again concluded that prevention of sorption of water within germanosilicate Ge-CIT-13 certainly inhibits the transformation.

7.3.3. Characterization of Resultant Ge-CIT-5

The physicochemical properties of the resultant Ge-CIT-5 obtained from the transformation of Ge-CIT-13 were further studied on the basis of the ^{29}Si solid-state NMR spectroscopy, argon adsorption isotherms (87.45 K), and computational chemistry.

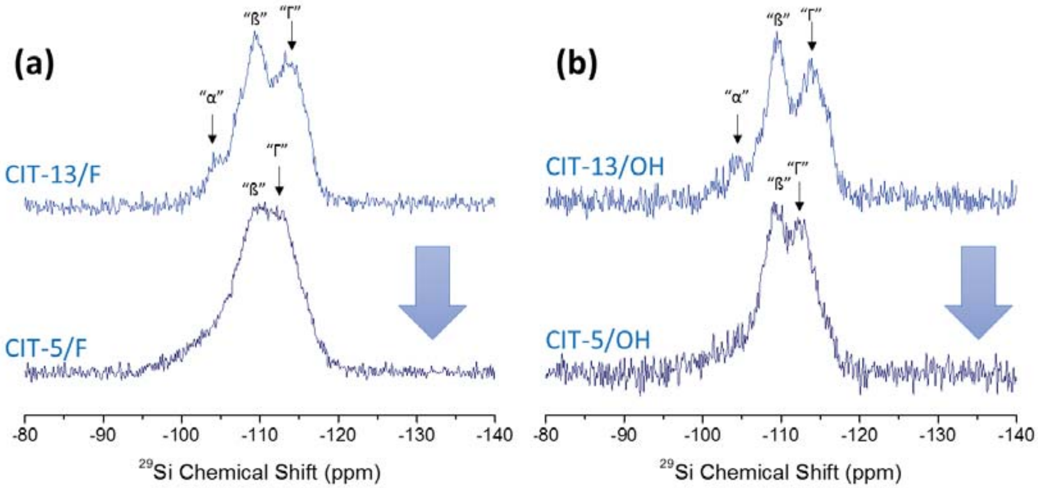

Figure 7.14. Transformation from (a) Ge-CIT-13/F[4.28] and (b) Ge-CIT-13/OH[3.87] and the resultant Ge-CIT-5's on the basis of 8 kHz MAS ^{1}H-decoupled ^{29}Si solid-state NMR spectra.

The ^{29}Si solid-state NMR spectra of freshly calcined Ge-CIT-13/F[4.28] and Ge-CIT-13/OH[3.87] and the resultant Ge-CIT-5 products from the two parent Ge-CIT-13 samples are illustrated in Figure 7.14. The studied germanosilicates were thoroughly dehydrated to eliminate possible influences of sorbed moisture and Q^3-silanol groups on ^{29}Si Bloch-decay NMR spectra by treating them under a dry air flow at 580 °C for 12 hours. The completeness of dehydration was confirmed by the absence of any peaks in the ^{1}H NMR and ^{1}H-^{29}Si CP-MAS NMR spectra (not shown). Deconvolution of ^{29}Si NMR spectra of typical extra-large-pore germanosilicates having many T-atoms such as CIT-13 is generally very complicated due to the presence of germanium and high-strain composite building units such as *d*4*r* units. These factors often make ^{29}Si NMR spectra of germanosilicates difficult to interpret in the range from -100 ppm to -120 ppm.[170, 191-192] But as one can see in Figure 7.14., calcined Ge-CIT-13 always shows three groups of peaks (denoted as "α", "ß", and "γ") at approximately -104 ppm, -109 ppm, and -114 ppm regardless of the type of mineralizers used to synthesize and Si/Ge ratios. There is a consensus that the most downfield peak α typically seen in the range from -102 ppm to -110 ppm originates from the Q^4-silicon in Ge-rich *d*4*r* units.[118, 178, 193] The other two groups ß and γ are assigned as the Q^4-silicon in Si-rich *cfi*-layers. After the transformation, group α peaks seemingly disappear since it is actually mixed with group ß peaks as a result of an upfield shift. This is a reasonable observation since the core part of the transformation from CIT-13 to CIT-5 is the dissembly-reassembly process from arrays of *d*4*r* units to double zigzag chains. Peak group "ß" showed no chemical shift change after the transformation. However, peak group γ slightly moved toward downfield from -114 ppm to -112 ppm after the transformation. These downfield-shifts were observed in the transformations of both Ge-CIT-13/F[4.28] and Ge-CIT-13/OH[3.87].

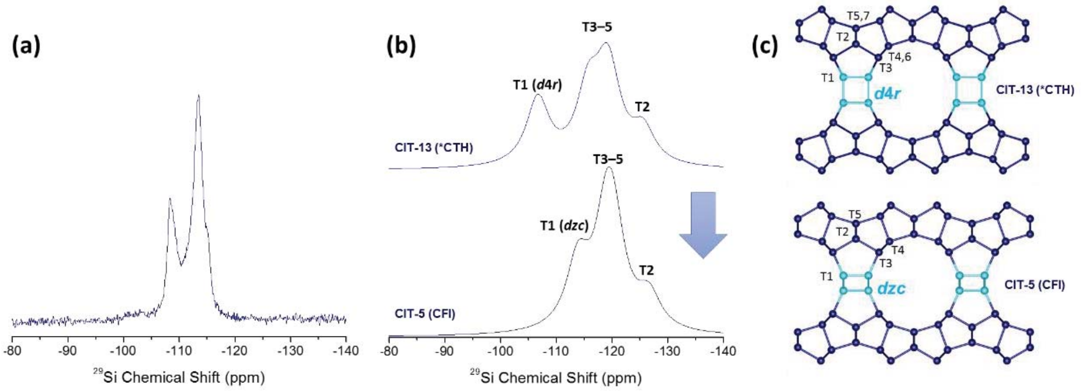

Figure 7.15. NMR spectroscopy and transformation. (a) 8 kHz MAS ^1H-decoupled ^{29}Si solid-state NMR spectrum of the reference Spa-CIT-5. (b) Calculated ^{29}Si NMR spectra of theoretical pure-silica molecular sieves having CIT-13 and CIT-5 topologies. (100% Lorentzian, width = 5.08 ppm) (c) Frameworks of CIT-13 and CIT-5 seen from the 14-ring channel direction with T-atom labels.

To further study the origins of these peak groups, estimated signal positions of each T-atom in the two frameworks were calculated based on a theoretical model. Thomas and Klinowski et al. suggested the following empirical linear equation to estimate the chemical shifts of silicon atoms within pure silica tectosilicate frameworks: δ_{Si} (ppm) = -25.44 - 0.5793×$\theta_{T\text{-}O\text{-}T(avg)}$ (°) where δ_{Si} is the estimated chemical shift of a framework Si from TMS (0 ppm) and $\theta_{T\text{-}O\text{-}T(avg)}$ is the average of four T-O-T angles surrounding that Si atom.[194] For CIT-13, a structure solution based on the rotational electron diffraction (RED) experiment conducted by Dr. Dan Xie at Chevron was used. This solution was acquired from one of the first Ge-CIT-13 samples made in 2016.[63] For CIT-5, the structure refinement based on the synchrotron PXRD data published by the Davis group in 1998 was used.[132] All frameworks were assumed to be pure-silica. Estimated values of chemical shifts were also provided in Table B5.

The calculated ^{29}Si NMR spectra of hypothetical pure-silica *CTH and CFI-type zeolites are illustrated in Figure 7.15(b). The actual ^{29}Si NMR spectrum of pure-silica Spa-CIT-5 is also acquired and provided in Figure 7.15(a) for comparison. The obtained ^{29}Si spectrum of Spa-CIT-5 was within experimental error of the reported spectrum.[132] It also was found that the empirical equation by Thomas et al.[194] apparently overestimates the magnitude of magnetic shielding in these extra-large-pore molecular sieves. In the calculated spectra, it can be easily noticed that there are also three groups of T-atoms in the frameworks of CIT-13 and CIT-5, as observed in those of germanosilicates shown in Figure 7.14, even though the presence of Ge-O-Si bonds broadens and moves ^{29}Si signals toward further downfield.[192] The first groups are groups of T-atoms involved in layer-connecting composite building units which are the *d*4*r* and *dzc* units in CIT-13 and CIT-5 frameworks, respectively. There is only one crystallographically distinguishable T-atom site (denoted as T1 in Figure 7.15(c)) in each of frameworks in the first group. The estimated positions of the first group T-atoms in ^{29}Si NMR spectra were -106.7 ppm (*d*4*r* in CIT-13) and -113.9 ppm (*dzc* in CIT-5). As expected, this explains the “disappearance” of the peak group α in Figure 7.14 (a) and (b).

The second group is a group of T-atoms which are not directly exposed to pores (denoted as T2). Four oxide ions which are directly connected to this T2-site, are not exposed to the channel system either. This T-site appeared at the most upfield positions (-125.6 ppm for CIT-13, -126.7 ppm for CIT-5) in the theoretical spectra due to its high T-O-T angles. But, these estimated positions fail to explain the downfield shift of the peak group γ in the actual spectra. The last group is a group of T-atoms (T3–5 for CIT-5, and T3–7 for CIT-13) forming the rest of 14-ring channel walls of CIT-13 and CIT-5. This third group of T-atoms can be assigned as the group ß peaks in the actual spectra based on their unmoved positions. In conclusion, the downfield shift of the peak group γ could not be explained on the basis of the Thomas empirical equation. I believe that there must be some influences of neighboring germanium atoms which are not considered in this model.

The microporosity of the related germanosilicates were studied based on the argon adsorption isotherms acquired at 87.45 K. The isotherms of as-calcined Ge-CIT-13/F[4.22], the resultant Ge-CIT-5, and the reference pure-silica Spa-CIT-5 are illustrated in Figure 7.16 in (a) linear scale and (b) log scale. As a result of the transformation, the estimated micropore volume was decreased from 0.169 cc g^{-1} (Ge-CIT-13) to 0.079 cc g^{-1} (Ge-CIT-5). On the other hand, the micropore volume of the reference Spa-CIT-5 was 0.091 cc g^{-1} which is 15 % higher than the isostructural Ge-CIT-5. The difference between the unit cell formula weight of Ge-CIT-5 and that of Spa-CIT-5 explains this micropore volume difference; the unit cell formula weight of Ge-CIT-5 having a Si/Ge ratio 4.22 (2.20 kg mol^{-1}, $Si_{25.9}Ge_{6.1}O_{64}$) is approximately 14 % heavier than that of pure silica CIT-5 (1.92 kg mol^{-1}, $Si_{32}O_{64}$). The unit-cell specific micropore volumes of Ge-CIT-5 and Spa-CIT-5 were 173 cc (mol of UC)$^{-1}$ and 175 cc (mol of UC)$^{-1}$, respectively, which are almost identical to each other.

In the log scale plot, a low-pressure adsorption behavior of Ge-CIT-5 was observed. Ge-CIT-13/F[4.22] and Spa-CIT-5, which are molecular sieves prepared directly from hydrothermal syntheses, started to adsorb argon at ca. $p/p_0 \sim 10^{-4}$. But Ge-CIT-5, which is a resultant material of transformation, started its argon uptake at ca. $p/p_0 \sim 10^{-5}$. As shown in Figure B12, the smaller-pore frameworks with higher-curvature surfaces uptake gas at lower partial pressures. It can be also concluded that this lower-pressure adsorption indicates the presence of higher-curvature surfaces which are presumably due to structural disorder caused during the transformation.

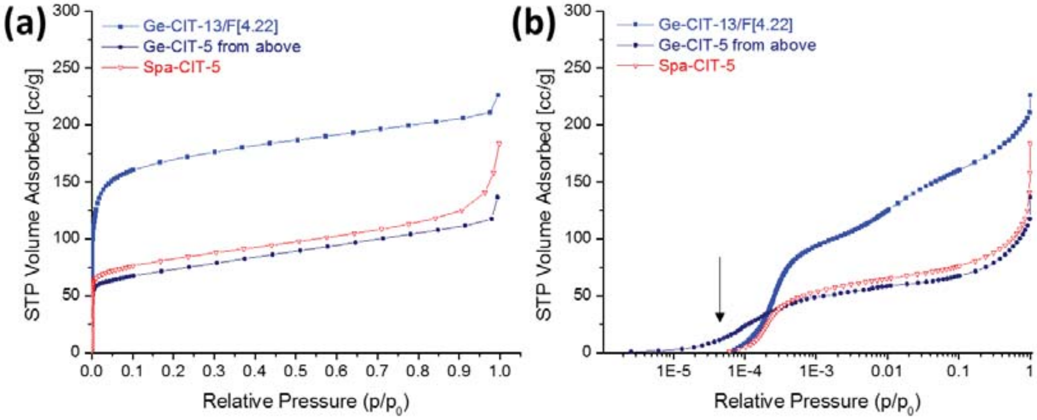

Figure 7.16. Argon adsorption isotherms (87.45 K) of Ge-CIT-13/F[4.22] and the resultant Ge-CIT-5 compared to the reference Spa-CIT-5. (“↓” denotes the low-pressure adsorption of Ge-CIT-5)

Lastly, the transformation was computationally investigated in terms of the lattice energy. It is reasonable to think that the major driving force of the transformation must be the high framework energy of CIT-13, particularly due to the high strain caused by the presence of *d*4*r* units. The lattice energies of CIT-13 and CIT-5 frameworks were calculated in the pure-silica and germanosilicate (Si/Ge = 3) systems. The models are shown in Figure 7.17. The computation was performed by Dr. Dan Xie at Chevron. For the pure-silica and germanosilicate computation, the GULP algorithm with the Catlow parameters and the FORCITE program with the COMPASS forcefield parameters were adopted, respectively, because the Catlow library used in the former module had no parameter relevant to germanosilicates. In the pure-silica system, the lattice energies of SiO_2-CIT-13 and SiO_2-CIT-5 relative to the α-quartz phase were +16.90 kJ mol^{-1} and +13.34 kJ mol^{-1} per Si-atom, respectively. The SiO_2-CIT-5 lattice model was more stable than that of SiO_2-CIT-13 by $\Delta U = -3.56$ kJ mol^{-1} per Si-atom mostly due to the high steric energy caused by *d*4*r* units.

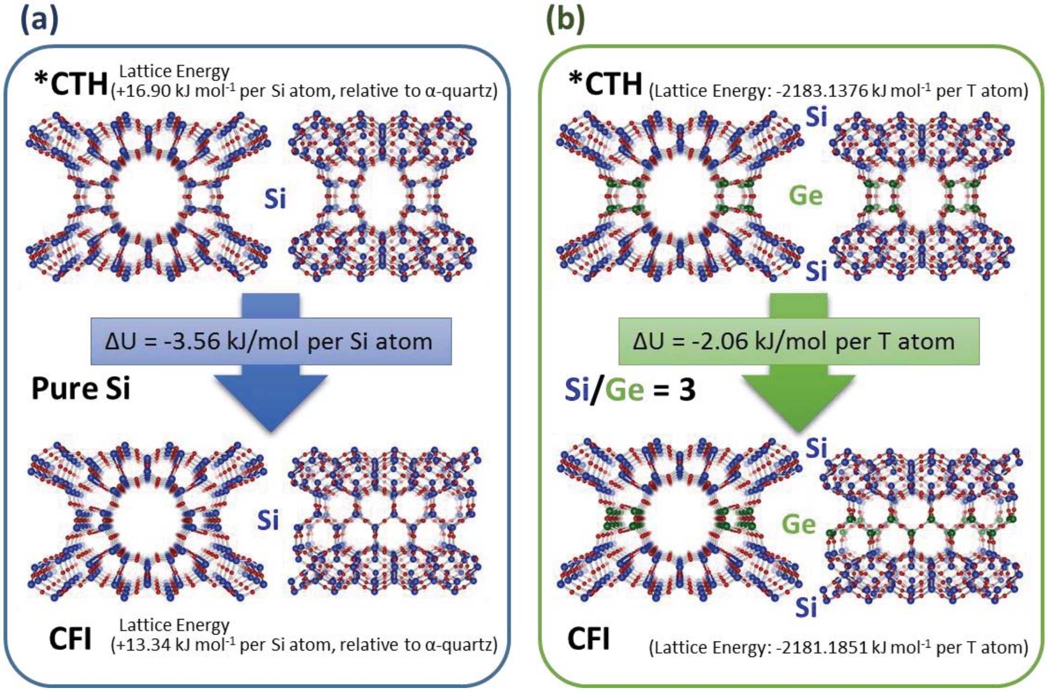

Figure 7.17. The lattice models used to calculate lattice energies: (a) pure-silica *CTH and CFI, and (b) hypothetical germanosilicate (Si/Ge = 3) crystal models of *CTH and CFI whose *cfi*-layers are exclusively composed of pure silica and whose connecting units—*d*4*r* and *dzc*—are completely composed of germanium oxide.

For the case of germanosilicates, two hypothetical germanosilicate Ge-CIT-13 and Ge-CIT-5 consisting of pure-silica *cfi*-layers and pure-germania *d*4*r* and *dzc* units (Si/Ge = 3 for both), respectively, were investigated. (Figure 7.17(b)) The calculated lattice energy difference between Ge-CIT-13 and Ge-CIT-5 was $\Delta U = -2.06$ kJ mol^{-1} per T-atom. Although detailed information about intermediate stages (i.e., activation energy, etc.) of this transformation are not clear yet, these computational results support that the transformation from CIT-13 to CIT-5 is energetically favorable and that it can be spontaneous if a proper condition is provided.

7.3.4. Comparison to Related Germanosilicate

Germanosilicates consisting of chemically stable silicate layers pillared with Ge-rich *d*4*r* units have attracted tremendous interest from the scientific society due to their ability to be transformed into novel structures. The most extensively studied framework is UTL.[117, 119] A number of novel microporous frameworks were prepared on the basis of transformation of UTL-type germanosilicates.[118, 122-123, 161-162] This family of frameworks includes IWW, ITH, ITR, IWR, and UOV.[195]

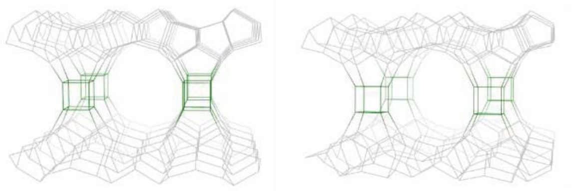

CIT-13 (***CTH**) IM-12, ITQ-15 (**UTL**)

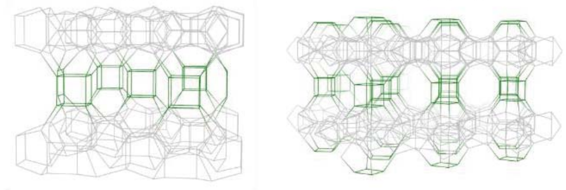

ITQ-13, JLG-18 (**ITH**) ITQ-22 (**IWW**)

Figure 7.18. Structures of germanosilicates consisting of Ge-rich *d*4*r* units and Si-rich layers.

In this section, how structures of these germanosilicates evolve upon exposure to moisture in ambient air is discussed. Among the frameworks enumerated above, the three most frequently studied frameworks—UTL, ITH, and IWW—were selected and investigated. Figure 7.18 demonstrates the structures of these topologies together with CIT-13. UTL is a "sister" framework of CIT-13 whose two dimensional channel system is defined by 14- and 12-ring. ITH is a medium-pore germanosilicate that has a staggered arrangement of *d*4*r* units in the interlayer region.[149] IWW has a very interesting 3-dimensional channel system consisting of perpendicularly intersecting 12-, 10-, and 8-ring pores.[146] For all of these frameworks, efforts have been made to hydrothermally stabilize these germanosilicates on the basis of many postsynthetic treatments.[154, 158-159, 196]

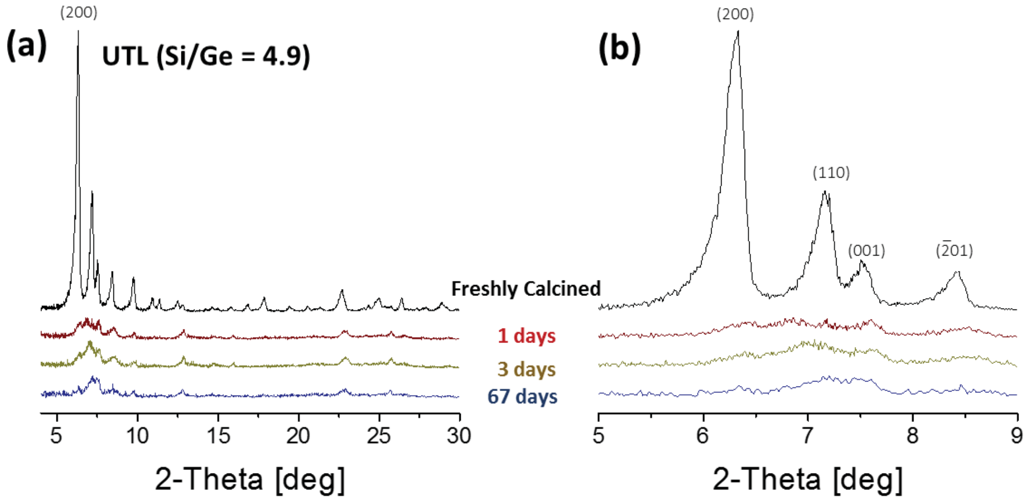

Figure 7.19. Structural change of IM-12/OH (Si/Ge = 4.9) over time observed on the basis of PXRD patterns in 2-theta scanning ranges of (a) 4–30° and (b) 5–9°.

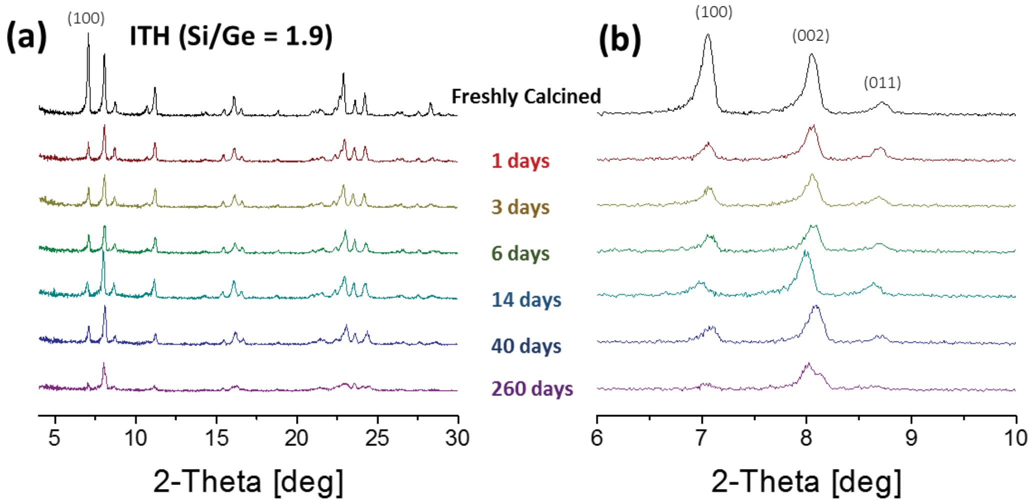

Figure 7.20. Structural change of JLG-18/F (Si/Ge = 1.9) over time observed on the basis of PXRD patterns in 2-theta scanning ranges of (a) 4–30° and (b) 6–10°.

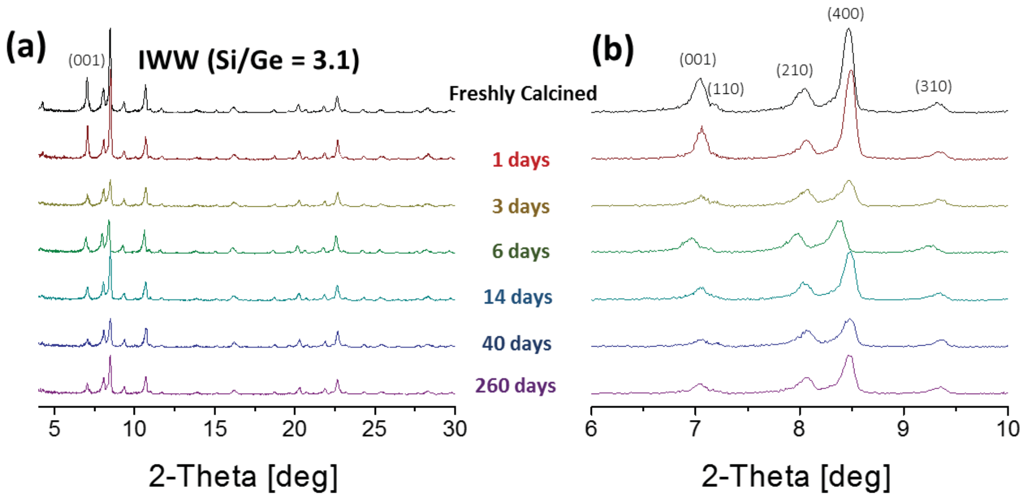

Figure 7.21. Structural change of ITQ-22/OH (Si/Ge = 3.1) over time observed on the basis of PXRD patterns in 2-theta scanning ranges of (a) 4–30° and (b) 6–10°.

In this work, IM-12,[116] JLG-18,[185] and ITQ-22[146] germanosilicates having UTL, ITH, and IWW frameworks, respectively, were prepared. Following the same nomenclature used for a series of parent CIT-13 samples in the previous sections of this chapter, each sample was also named as "*material name"/mineralizer[Si/Ge ratio]*. For example, ITQ-22/OH[3.5] denotes an ITQ-22 germanosilicate sample having a Si/Ge ratio of 3.5 which was synthesized from hydroxide media.

Instead of being transformed into another frameworks, IM-12/OH[4.9] simply lost its crystallinity rapidly as shown in Figure 7.19. After 1-day exposure to ambient humidity, the initial UTL structure completely disappeared. No further structural change was observed in this collapsed structure during the following 67 days of extended observation. Contrary to the case of UTL, JLG-18/F[1.9] and ITQ-22/OH[3.1] showed almost no structural change. (Figures 7.20. and 7.21) These structures were stable despite their low Si/Ge ratios. After 260 days of exposure, JLG-18/F[1.9] lost most of its crystallinity, but still retained its original framework. ITQ-22/OH[3.1] showed no significant structural degradation even after 260 days of exposure to moisture.

The fragility of UTL germanosilicates can be explained by its most opened structure and unique arrangement of germanium atoms in its *d*4*r* units. UTL has the lowest framework density (15.6 T-atoms nm^{-3}) and largest pore opening (14×12) among all studied frameworks in this chapter. Water molecules from the atmosphere may have rapidly reached the deepest part of the UTL framework and hydrolyzed Ge-O bonds which are well exposed to the surrounding large- and extra-large-pore channel system. The distance between neighboring two *d*4*r* units is too far to achieve the CIT-13-like transformation by forming new Ge-O-T bonds. The 2-dimensional arrangements of *d*4*r* units within the interlayer region of germanosilicates are illustrated in Figure B18. The closest distance between two neighboring *d*4*r* units in UTL is 6.04 Å which is much longer than that of CIT-13 (3.63 Å). Instead, UTL-type germanosilicates could undergo a novel type of transformation based on the shift of layers by half the unit-cell vector along the 14-ring channel direction thanks to this geometry, yielding two new topologies, IPC-9 and IPC-10 having 2-dimensional 10/7-ring and 12/9-ring channel systems, respectively.[162]

The unique arrangement of germanium T-atoms within *d*4*r* units may be another reason for the hydrothermal instability of UTL. UTL had been the only germanosilicate that can undergo the inverse sigma transformation[118] before I discovered that Ge-CIT-13/OH has the same ability (shown in the next chapter) to transform. The existence of single-4-ring (*s*4*r*) configuration of germanium T-atoms within the *d*4*r* units is an indispensable condition for this type of direct transformation.[118, 176] The presence of Ge-O-Ge bonds within *d*4*r* units may have seriously weakened the framework in terms of hydrolysis by sorbed moisture.

ITH also have a long distance (5.53 Å) between parallel pairs of neighboring *d*4*r* units, and IWW has no parallel pair of neighboring *d*4*r* units as shown in Figure B18. The high hydrothermal stability of ITQ-22 was reported many times.[176] Delamination and reassembly of Ge-rich ITQ-22 resulted in the restoration of initial IWW framework.[197] Xu et al. reported that, even after complete removal of germanium from germanosilicate ITQ-22 by soaking the material in strong acid, the IWW framework was retained.[154] On the basis of delamination and relevant NMR studies, Kasian et al. concluded that the high stability of ITQ-13 (ITH) and ITQ-22 is due to their arrangements of Ge and Si T-atoms within *d*4*r* units which is vastly different to that of UTL.[176]

7.4. Summary

The kinetics of the transformation from Ge-CIT-13 to Ge-CIT-5 was closely related to the nature of the parent Ge-CIT-13. Apparently, Ge-CIT-13 with a higher germanium content was transformed faster than Ge-CIT-13 with a lower germanium content.

Interestingly, it was found that the type of mineralizer which was used to synthesize the parent CIT-13 immensely influenced the rate of transformation. Ge-CIT-13 synthesized from the fluoride-free recipe was transformed into Ge-CIT-5 much faster than Ge-CIT-13 crystallized in fluoride media. A Ge-CIT-13 sample synthesized in hydroxide media having a low Si/Ge ratio of 3.88 was completely transformed into Ge-CIT-5 within a couple of days.

Isolating Ge-CIT-13 from the presence of moisture inhibited the transformation. All measures which excludes sorption of water within the pore system of Ge-CIT-13 including dry argon mood, hydrophobic cyclohexane adsorption, and storage temperature higher than the boiling point of water significantly decelerated the transformation. These observations strongly evidence that the presence of sorbed water is indispensable for the transformation of Ge-CIT-13 to Ge-CIT-5.

The properties of resultant Ge-CIT-5 were investigated. In argon adsorption, a small degree of disorder was observed in the low pressure region presumably formed during the transformation. However, the overall microporosity matched well with pure-silica CIT-5. In the ^{29}Si NMR spectra, disappearance of *d*4*r* signals was observed. But other evolutions in the ^{29}Si NMR spectra could not fully be explained with the currently available experimental results. The structural changes of other germanosilicates having *d*4*r* units were also investigated. While UTL completely collapsed within a day, ITH and IWW retained their original structures relatively well. No significant diffraction shift was observed in these materials. Ge-CIT-13 remained as the only germanosilicate to date which undergoes this type of transformation.